JBC Papers in Press. Published on June 26, 2017 as Manuscript M117.794339
The latest version is at http://www.jbc.org/cgi/doi/10.1074/jbc.M117.794339

Deciphering the role of the signal- and Sty1 kinase-dependent phosphorylation of the stress-responsive transcription factor Atf1 on gene activation

Clàudia Salat-Canela[1], Esther Paulo[1], Laura Sánchez-Mir[1], Mercè Carmona[1], José Ayté[1], Baldo Oliva[2], and Elena Hidalgo[1]

[1]From the Oxidative Stress and Cell Cycle Group, and [2]Structural Bioinformatics Laboratory (GRIB), Universitat Pompeu Fabra, C/ Dr. Aiguader 88, 08003 Barcelona, Spain

Running title: *Activation of Atf1 by phosphorylation*

To whom correspondence should be addressed: Elena Hidalgo, Address correspondence to: Elena Hidalgo, Universitat Pompeu Fabra, C/ Dr. Aiguader 88, 08003 Barcelona, Spain, Telephone: 34-93-316-0848; FAX: 34-93-316-0901; E-mail: elena.hidalgo@upf.edu

The first three authors contributed equally to this work

Keywords: transcription regulation / *Schizosaccharomyces pombe* / phosphorylation / Sty1 / Atf1 / oxidative stress

ABSTRACT

Adaptation to stress triggers the most dramatic shift in gene expression in fission yeast (*Schizosaccharomyces pombe*), and this response is driven by signaling via the MAPK Sty1. Upon activation, Sty1 accumulates in the nucleus, and stimulates expression of hundreds of genes via the nuclear transcription factor Atf1, including expression of *atf1* itself. However, the role of stress-induced, Sty1-mediated Atf1 phosphorylation in transcriptional activation is unclear. To this end, we expressed Atf1 phosphorylation mutants from a constitutive promoter, to uncouple Atf1 activity from endogenous, stress-activated Atf1 expression. We found that cells expressing a nonphosphorylatable Atf1 variant are sensitive to oxidative stress because of impaired transcription of a subset of stress genes whose expression is controlled also by another transcription factor, Pap1. Furthermore, cells expressing a phosphomimicking Atf1 mutant display enhanced stress resistance, and while expression of the Pap1-dependent genes still relied on stress induction, another subset of stress-responsive genes was constitutively expressed in these cells. We also observed that in the cells expressing the phosphomimicking Atf1 mutant, the presence of Sty1 is completely dispensable, with all stress defects of Sty1-deficient cells being suppressed by expression of the Atf1 mutant. We further demonstrated that Sty1-mediated Atf1 phosphorylation does not stimulate binding of Atf1 to DNA, but rather establishes a platform of interactions with the basal transcriptional machinery to facilitate transcription initiation. In summary, our results provide evidence that Atf1 phosphorylation by the MAPK Sty1 is required for oxidative stress responses in fission yeast cells and by promoting transcription initiation.

Several mitogen-activated protein (MAP) kinase pathways allow eukaryotic organisms to respond to environmental challenges by triggering stress-dependent gene expression programs. Upon exposure to signals, phosphorylated MAP kinase accumulates in the nucleus and triggers phosphorylation of transcription factors (TFs). The activated TFs are then able to translate extracellular cues into specific cellular responses, by adapting the complex RNA polymerase II (Pol II) transcriptional machinery into particular sets of genes and mediate specific changes in the gene expression program (1).

The fission yeast *Schizosaccharomyces pombe* responds to environmental stressors by inducing a complex signal transduction pathway

meant to allow survival: the Sty1/Spc1 MAP kinase pathway. The pathway is induced by many stress conditions, and triggers a wide transcriptional shift of the gene expression program (2,3). A common consequence of the different signals is the activation by phosphorylation of the MAP kinase Sty1 (4,5). Then Sty1 transiently accumulates in the nucleus, where it promotes transcriptional activation or repression of genes in an, at least partially, Atf1-dependent manner (4,6-8). Atf1 is a basic zipper (bZIP)-containing TF which heterodimerizes with another bZIP protein called Pcr1; even though the phenotypes of cells lacking one or another TF are not identical, they have overlapping functions (9,10), and Atf1 seems to be the direct substrate of the MAP kinase Sty1 (8). Sty1 phosphorylation is required to trigger both nuclear accumulation as well as activation of its kinase activity, since constitutive nuclear accumulation of the kinase is not sufficient to induce phosphorylation of its main substrate, Atf1, nor to activate transcription (9,11). In response to toxic but not lethal extracellular hydrogen peroxide (H_2O_2), more than 500 genes are up-regulated more than two-fold. Their induction depends on Sty1 and, to a lesser extent, on Atf1 (2,3). Even though a lot of work has been done to identify and characterize the downstream effectors of activated Sty1-Atf1 on transcription regulation, such as the SAGA complex (12), it is not clear which is the main role of the Sty1 kinase activity on the Pol II-dependent transcription of stress genes. A first possibility, based on the ortholog kinase HOG1 of *Saccharomyces cerevisiae* [for a review, see (13)], is that the kinase participates directly on transcription initiation and/or even elongation; in this model, the MAP kinase Sty1 would only use Atf1 as an anchor to the stress promoters (10,14,15), where activated Sty1 could regulate the access or activity of the transcriptional machinery through phosphorylation of unknown substrate(s). A second proposal is that nuclear and activated Sty1 enhances, by phosphorylating Atf1, the affinity of the TF for its cyclic AMP response element (CRE) sites at stress promoters: only phosphorylated Atf1 would display low dissociation constants towards the CRE sites; while a genome-wide study using ChIP-sequencing of total immuno-precipitated Atf1 indicates that there is a significant enhancement of the TF binding to DNA upon activation by Sty1 (16), chromatin immuno-precipitation (ChIP) of individual stress genes reported a very modest recruitment, if any, of Atf1 to specific stress promoters upon stress imposition (9,15). Finally, it has also been proposed that the main role of Sty1 at promoting Atf1 function is by inhibiting its ubiquitin-dependent degradation (10,17), so that stabilization and accumulation of Atf1 upon phosphorylation would be the gene activation triggering event; in this case, enhanced TF concentration would increase promoter occupancy.

Another important aspect of this regulatory cascade is that the *atf1* gene is also up-regulated upon stress as part of a feedback loop. Thus, oxidative stress triggers transcription of this gene four-fold (2,3), which may contribute to enhancing Atf1 protein levels after stress. Thus, we decided to perform a characterization of the role of Sty1-dependent Atf1 phosphorylation by expressing from a constitutive promoter HA-tagged wild-type Atf1 and several mutants lacking some of the eleven serine/threonine-proline (S/TP) phospho sites. We demonstrate here that the transcriptional profile of *Δatf1* cells expressing HA-Atf1 is very similar to that of wild-type cells, despite the fact that the concentration of the TF is constant. Cells expressing Atf1 mutants lacking the S/TP sites are unable to trigger transcription of a subset of stress genes, while Atf1 mutants with substitutions mimicking phosphorylation are able to trigger constitutive or inducible transcription of the stress genes in a Sty1-independent manner.

RESULTS

Expression of Atf1 from a constitutive promoter does not alter the pattern of activation of stress genes - The *atf1* mRNA is up-regulated four-times upon H_2O_2 exposure in an Atf1-dependent manner (2). We expressed HA-Atf1 under the control of the constitutive promoter *sty1*; the gene chimera, coding for HA-Atf1 containing the eleven MAP kinase phosphorylation sites (Fig 1A), was integrated at the *leu1* locus of cells lacking Atf1. Expression of the HA-Atf1 chimera suppresses the

sensitivity to peroxides of cells deficient in Atf1 on solid plates (Fig 1B). As shown by Western blot, a shift in electrophoretic mobility, due to stress-dependent phosphorylation by Sty1 (7), can be detected for endogenous Atf1 and for HA-Atf1 (Fig 1C). Importantly, the use of anti-HA antibodies demonstrates that the levels of HA-Atf1 are not enhanced upon stress, as would be expected if phosphorylation would stabilize Atf1 (Fig 1C). Our study highlights that the use of polyclonal antibodies against Atf1 is not a reliable tool to perform relative quantifications of the TF in protein extracts, since polyclonal antibody recognizes with variable affinities the phosphorylated and unphosphorylated forms of wild-type HA-Atf1 (compare the intensities of the bands corresponding to HA-Atf1 before and after stress using anti-Atf1 or anti-HA; Fig 1C); similar observation has been reported previously for other antibodies [i.e.anti-retinoblastoma; (18)]. As shown with Northern blot, the Sty1-, Atf1-dependent gene expression program is engaged in the presence of peroxides in *Δatf1* cells expressing the HA-Atf1 chimera, as demonstrated with the activation of genes such as *srx1, ctt1, gpd1* or *hsp9*, coding for sulfiredoxin, catalase, glycerol-3P-dehydrogenase and heat shock protein 9, respectively (2) (Fig 1D). From these experiments, we conclude that Atf1 stabilization by phosphorylation is not the mechanism activating the TF.

Cells expressing an Atf1 mutant lacking ten out of eleven putative MAP kinase phosphorylation sites are sensitive to oxidative stress - We then tested the effect of phospho site substitutions on the activity of the TF. As shown in Fig 1A, ten of the eleven sites are located in the first half of Atf1. We synthesized chimeric genes coding for HA-Atf1.11M, HA-Atf1.10M and HA-Atf1.1M (Fig S1A), to render hypophosphorylation mutants (serine or threonine sites were mutated to alanine or isoleucine to avoid phosphorylation). As shown by Western blot in Fig S1B, the HA-Atf1.1M mutant displays an apparent shift in electrophoretic mobility in extracts from stressed cells identical to the wild-type protein, while the HA-Atf1.10M and HA-Atf1.11M (not shown) proteins did not seem to have a significant change in mobility. Concomitantly, while the HA-Atf1.1M mutant was fully able to suppress the sensitivity to peroxides of strain *Δatf1*, expression of the HA-Atf1.10M and 11M mutants did not alleviate this phenotype (Fig S1C). We then constructed a chimeric gene coding for HA-Atf1.10D, to render a phospho-mimicking mutant (serine or threonine sites were mutated to aspartic or glutamic acid to mimic phosphorylation) (Fig 1E). As shown by Western blot for HA-Atf1.10M, HA-Atf1.10D protein did not display any detectable mobility shift upon stress (Fig 1F). Concomitantly, while expression of HA-Atf1.10M was not able to suppress the sensitivity to peroxides of strain *Δatf1* (Fig S1C and Fig 1G), expression of HA-Atf1.10D alleviated this phenotype (Fig 1G).

We introduced lower number of substitutions in Atf1 to try to determine exactly which modification/s was/were essential for the role of Atf1 in oxidative stress survival. As shown in Fig S2, strain *Δatf1* expressing the mutant named HA-Atf1.6M, lacking the sites five-to-ten in Atf1, was as sensitive to grow on peroxide-containing plates as cells lacking Atf1. Therefore, residues Ser152, Ser172, Thr204, Thr216, Ser226 and Thr249 are essential for Atf1 function on oxidative stress survival.

Analysis of the transcriptional activity of the Atf1 phosphorylation mutants – characterization of two subsets of stress genes - We then tested how transcription of stress genes was affected in cells expressing the phospho Atf1 mutants. As shown by Northern blot in Fig 2A, cells expressing the hypo-phosphorylation mutant HA-Atf1.10M are not able to fully trigger the *ctt1* and *srx1* genes after H_2O_2 stress, while only minor defects are observed regarding activation of *hsp9* and *gpd1* (Fig 2A). Therefore, the impaired activation of only a subset of genes in cells expressing the Atf1.10M mutant, including that encoding catalase, causes a severe defect in tolerance to oxidative stress; this is in agreement with our previous observation indicating that *Δctt1* cells are as sensitive to peroxides as *Δatf1* cells and that over-expression of just catalase is sufficient to totally suppress the sensitivity to peroxides of cells lacking Atf1 (19). Expression of the phospho-mimicking HA-Atf1.10D mutant

allows stress-dependent activation of *ctt1* and *srx1* to the same extent as wild-type cells; however, it constitutively induces expression of *gpd1* and *hsp9* (Fig 2A).

To analyze the role of the MAP kinase Sty1 in the activation of stress genes by the HA-Atf1.10M and HA-Atf1.10D mutants, we expressed them in cells lacking Sty1. As shown in Fig 2B, the capacity of HA-Atf1.10M to activate *hsp9* and *gpd1* after stress imposition was abolished in the absence of Sty1, while the expression of all the stress genes in cells expressing HA-Atf1.10D was not altered by *sty1* deletion. Concomitantly, while wild-type HA-Atf1 and the hypo-phosphorylation mutant HA-Atf1.10M were not able to restore wild-type tolerance to H_2O_2, expression of HA-Atf1.10D fully suppressed all the stress defects of cells lacking Sty1 (Fig 2C). From these results we conclude that phosphorylation of Atf1 is sufficient for the constitutive activation of a subset of genes, such as *hsp9* and *gpd1*, while the expression of others (*ctt1* and *srx1*) is still dependent on stress imposition. Importantly, expression of the phospho-mimicking HA-Atf1.10D (Fig 2B) or HA-Atf1.6D (Fig S3CD) bypasses the requirement for a MAP kinase in the transcription process, which questions the direct participation of the kinase on Pol II initiation and/or elongation.

Since H_2O_2 treatment induces over two-fold the expression of hundreds of genes in wild-type cells in a Sty1-dependent manner (2), we tested whether expression of HA-Atf1.10D in strain *Δsty1* affects the whole oxidative stress-dependent gene expression program. We analyzed by RNA-sequencing the global transcriptome of wild-type and *Δsty1* cells, as well as of Δ*sty1* expressing HA-Atf1, HA-Atf1.10D or HA-Atf1.10M. As shown in Fig 2D and in Table S1 , most of the stress genes activated after 15 min of 1 mM H_2O_2 in a wild-type background are not inducible in a *Δsty1* background, and in fact their basal expression levels in this strain are significantly lower than in wild-type cells. Expression of HA-Atf1 or HA-Atf1.10M did not affect this pattern of expression of cells lacking Sty1. However, in *Δsty1* cells expressing HA-Atf1.10D more than half of the stress genes displayed up-regulation by stress more than 1.5-fold (*ctt1* and *srx1* are indicated with arrows in Fig 2D), while half of the remaining genes displayed basal expression levels higher than 1.5-fold (similar to *hsp9* and *gpd1,* also indicated in Fig 2D). We conclude that HA-Atf1.10D significantly affects the gene expression pattern of strain Δ*sty1*.

Recruitment of Atf1 to stress promoters is not dependent on its phosphorylation by Sty1 - Since Atf1 displays constitutive nuclear localization, we aimed at determining whether the phosphorylation-driven event was to promote Atf1 binding to DNA. We first attempted to perform ChIP with our constitutively expressed HA-Atf1 mutants, but the amino-terminal HA tag was probably hindered for antibody recognition during ChIP experiments. We decided to add the tags at the carboxi-terminal domain of Atf1 at the endogenous *atf1* locus.

We first mutated seven central S/TP sites, rendering cells expressing Atf1.7M and Atf1.7D under the control of the endogenous *atf1* promoter (Fig S4A). Strains expressing wild-type Atf1 or Atf1.7M or Atf1.7D mutants displayed the same patterns of tolerance to peroxides and activation of stress genes as the constitutive amino-terminal tagged versions (Fig S4BC). We then introduced HA-tags at the carboxi-terminal-coding regions of the *atf1, atf1.7M* and *atf1.7D* chromosomal loci. Cells expressing the tagged Atf1 proteins displayed the expected tolerance to peroxides and gene expression profiles; the mutant proteins displayed the expected electrophoretic mobilities (Fig S4DEF).

We analyzed by ChIP the presence of wild-type Atf1-HA and phospho mutant derivatives at promoters of stress genes before and after H_2O_2. As shown in Fig 3A, Atf1-HA, Atf1.7D-HA and Atf1.7M-HA are constitutively bound to the *gpd1* and *hsp9* promoters, both before and after stress. Regarding the binding of wild-type and mutant Atf1-HA to the *ctt1* and *srx1* promoters, the TF seems to be pre-bound under basal conditions relative to control primers, but three-to-four fold additional recruitment is detected after stress imposition (Fig 3A). Importantly, the patterns of recruitment of Atf1, Atf1.7D and Atf1.7M to stress promoters are very similar, indicating that

the presence of Atf1 at promoters by itself is not sufficient to explain the transcriptional induction of stress genes.

We reported that the recruitment of Pol II at stress genes is stress-dependent, with accumulation of the polymerase subunits Rpb1 or Rpb3 at their open reading frames after stress imposition (12). To confirm that active Atf1 favors recruitment of active Pol II at stress genes, we analyzed by ChIP the presence of the Pol II subunit Rpb3 at the *ctt1* and *gpd1* promoters, open reading frames and 3'-untranslated regions in cells expressing wild-type Atf1, Atf1.7D or Atf1.7M. As shown in Fig 3BC, the presence of Pol II at bodies of stress genes correlates with the transcription profiles of cells expressing wild-type and mutant Atf1.7D or Atf1.7M (compare Fig 3BC with Fig S4C). From these ChIP experiments we conclude that the stress-dependent phosphorylation of Atf1 does not facilitate its recruitment to DNA, but rather promotes directly or indirectly Pol II recruitment to stress genes.

Role of other bZIP TFs, Pcr1 and Pap1, in the activation of stress genes - There are six TFs in *S. pombe* containing a bZIP DNA binding motif, three of which have been clearly connected to the environmental stress response: Atf1, Pcr1 and Pap1. Pcr1 has been shown to form a heterodimer with Atf1 and to contribute to some of its functions (20,21); however, the phenotypes and transcriptomes of strains lacking either Atf1 or Pcr1 do not fully overlap (9). As shown in Fig 4A, Pcr1 is only dispensable in the activation of *srx1* upon H_2O_2 stress, although its binding to stress promoters fully overlaps the binding of Atf1 (Fig 4B). The role of Pcr1 in the activation of Sty1- and Atf1-dependent transcription of genes such as *ctt1, gpd1* and *hsp9* resides probably in the recognition of Atf1-binding sites at promoters, which can only be accomplished when Atf1 is forming a heterodimer with Pcr1: expression of the Sty1-independent Atf1.7D-HA mutant cannot bypass the absence of Pcr1, as shown by the lack of transcription of stress genes (Fig 4C). Finally, we analyzed by ChIP whether Atf1 binding to DNA is dependent on the presence of Pcr1; as shown in Fig 4D, Atf1-GFP is not recruited to DNA in *Δpcr1* cells, with the only exception of *srx1*; as with untagged Atf1, *Δpcr1* cells expressing Atf1-GFP displayed defective activation of most stress genes except *srx1* (Fig S4G).

On the other hand, another bZIP TF, Pap1, specifically responds to H_2O_2 but not to other environmental signals, and some of its target genes overlap with those activated by Sty1-Atf1 (3); activation of Pap1 by H_2O_2 occurs through oxidation of several of its cysteine residues to disulfides, and transient nuclear accumulation due to nuclear export inhibition (22,23). We tested the contribution of this bZIP TF to the expression of the two Sty1-, Atf1-dependent subsets of genes by Northern blot, and determined that Pap1 is dispensable for the activation of *gpd1* and *hsp9* but is required for *ctt1* and *srx1* (Fig 5A). In fact, while HA-Atf1.10D is still capable of activating transcription of both subsets of genes in cells lacking Sty1, further depletion of Pap1 specifically abolishes the activation of *srx1* and *ctt1*, but maintains constitutive expression of *gpd1* and *hsp9* (Fig 5B).

Regarding the role of Pap1 and Atf1 at these genes, ChIP analysis indicates that the stress-dependent recruitment of Atf1 to *ctt1* and *srx1* promoters is dependent on Pap1 (Fig 5C). We recently reported that in cells lacking thioredoxin reductase (Trr1), Pap1 is constitutively oxidized and bound to *srx1* and *ctt1* even prior to stress, while the Pap1.C523D can never bind to these promoters even after stress imposition (24). Concomitantly, Atf1 is constitutively bound to *srx1* and *ctt1* in strain *Δtrr1*, while it is never recruited to these promoters in cells expressing Pap1.C523D (Fig 5D). Finally, the loading of Pap1 to *srx1* and *ctt1* is not impaired in the absence of Atf1 (Fig 5E). These results indicate that the binding of oxidized Pap1 to *srx1* and *ctt1* precedes and is required for the stress-dependent recruitment of Atf1.

DISCUSSION

In *S. pombe,* the Sty1 pathway coordinates a wide anti-stress gene expression program in response, among others, to severe H_2O_2 stress. The role of Atf1 phosphorylation by Sty1 was uncertain, as it had been proposed to be relevant

only as a protein stabilization factor. We dismiss here this hypothesis by showing that the protein levels of constitutively-expressed HA-Atf1 do not change upon stress imposition. We demonstrate that the main role of activated Sty1 is phosphorylating Atf1, since a phospho-mimicking Atf1 mutant is able to engage the anti-stress transcriptional program in a Sty1-independent fashion. We also show that phosphorylation of the TF does not contribute to Atf1 recruitment to DNA, but promotes transcription initiation.

Atf1 contains eleven putative sites of phosphorylation by Sty1. Amino acid substitutions of sites 5 to 10 (Ser152, Ser172, Thr204, Thr216, Ser226 and Thr249) are sufficient to render an inactive Atf1, since cells expressing HA-Atf1.6M are as sensitive to peroxides as strain *Δatf1* (Fig S3). We have modeled the structure of full-length Atf1 with the suite I-TASSER (25) to determine the relative position of these six phospho residues and the bZIP domain. According to this model (Fig 6), the DNA-binding domain and five of the six phospho sites (located at a putative transactivation domain) would be separated by an intermediate domain. The intermediate domain is rich in positively charged amino acids, supporting a role in promoting Atf1 binding to DNA and buffering the gain of negative charges due to phosphorylation at the transactivation domain. An important conclusion of the predicted structure of Atf1 is that the relative position of the five phospho residues surface is very distant from the DNA binding domain. This supports our experimentally-based data, where phosphorylation of Atf1 does not have an effect on binding capacity of Atf1 to DNA but rather may create an interacting platform to facilitate posterior events in the transcription initiation process, such as recruitment of SAGA complex or Pol II (12).

We have shown here that only a subset of genes, such as *ctt1* and *srx1*, are severely affected by the absence of these phospho sites at Atf1. We are still puzzled by the fact that the hypo-phosphorylation mutants are able to promote transcription of the second subset of genes (*gpd1* and *hsp9*) in a Sty1-dependent manner. We are investigating three possible scenarios: first, that Sty1 is phosphorylating a partner of Atf1, such as another bZIP TF; second, that Sty1, recruited to these promoters by HA-Atf1.10M or Atf1.7M, can also promote transcription activation; and third, that Sty1 can phosphorylate and activate Atf1 at either the five S/TP sites or at other non-canonical sites. Further work will be required to identify the target/s of Sty1 at these stress promoters when Atf1 lacks all these phosphorylation sites. Independently of the final outcome, we propose that Atf1 is constitutively bound to these promoters, and that phosphorylation of Atf1 by Sty1 is sufficient to promote transcription initiation, since the phospho-mimicking mutants (HA-Atf1.10D, HA-Atf1.6D, Atf1.7D) can bypass the presence of Sty1 and trigger constitutive transcription of these genes.

Transcription of the Pap1-dependent set of genes, such as *ctt1* and *srx1*, seems to follow a different pattern: a small fraction of these promoters are bound to Atf1 under basal conditions, as demonstrated by ChIP, even though this binding is significantly enhanced upon activation by stress. The stress-dependent new recruitment of Atf1 requires prior loading of Pap1, another bZIP TF which also becomes activated by H_2O_2, and it is independent of Atf1 phosphorylation status. Probably Pap1 and Atf1 synergistically contribute to full activation of these essential antioxidant genes, and full transcriptional up-regulation is only accomplished when both TFs are loaded onto DNA.

The presence or absence of Sty1 does not affect the transcriptional activity of HA-Atf1.10D, and this allows us to conclude that the main role of the MAP kinase at promoters is Atf1 phosphorylation. Therefore, the putative participation of Sty1 itself in the transcription process of the *S. pombe* stress genes (as a transcription initiation or elongation factor, as proposed for the *S. cerevisiae* homologue HOG1) is dismissed by our experiments. Furthermore, Sty1 and Atf1 have been described to participate in processes other than activation of stress genes (homologous recombination, heterochromatin establishment, regulation of the *ste11* and *fbp1* genes…) [for a review, see (26)]. Future experiments will show if the phospho-mimicking Atf1 mutants can complement the

absence of Sty1 in some or all of these biological functions.

EXPERIMENTAL PROCEDURES

Yeast strains, plasmids and growth conditions - Origins and genotypes of strains used in this study are outlined in Table S2. We used integrative plasmids p428' (27) and p428' mutant derivatives to express HA-Atf1 and HA-Atf1 phospho mutants under the control of the constitutive *sty1* promoter, most of which were generated by full length gene synthesis (Genescript), as previously described (27). The plasmids were linearized and integrated by homologous recombination in two strain backgrounds: strain EP193 (*atf1::natMX6)*, in which the entire *atf1* open-reading frame has been substituted by an antibiotic resistance cassette, and strain IV59 (*atf1::natMX6 sty1::ura4)*, with *ura4* insertion deleting codons 35-to-166 of the *sty1* open-reading frame. The mutant plasmids were inserted at the *leu1-32* locus of strains EP193 and IV59 yielding the EP203 series (*Δatf1* expressing HA-Atf1 or mutant derivatives) and the EP303 series (*Δatf1 Δsty1* expressing HA-Atf1 or mutant derivatives), respectively. To construct the strains EP201 and EP288, used as negative control, we integrated the p386' plasmid expressing only the *sty1* promoter fused to HA at the *leu1-32* locus of EP193 and IV59 strains, respectively. To generate strains expressing Atf1.7M and Atf1.7D under the control of its own promoter, we first deleted the *atf1* central region [deletion of codons 138 to 252 of *atf1* open reading frame (ORF)] in the strain JA364 (h^+ *ura4.D18*) with a cassette containing the *ura4+* gene, yielding strain MC117 (h^+ *atf1::ura4 ura4.D18*). Next, we replaced the mutated *atf1* gene by recombination with a linear fragment of the wild-type and mutant *atf1* ORF obtained by PCR (polymerase chain reaction) amplification with specific primers using p428' and mutant derivatives as templates. Then, we selected the uracil auxotrophic clones by resistance to 5-fluoroorotic acid (5-FOA; Toronto Research Chemicals Inc.) yielding strains MC119.7M and MC119.7D. To tag *atf1*, *atf1.7M*, *atf1.7D, rpb3* and *pcr1* with *HA* or *GFP*, we transformed strains 972, MC119.7M and MC119.7D with linear fragments containing the 3' end of the genes fused to *HA::natMX6* or *GFP::kanMX6*, obtained by PCR amplification using specific primers and the plasmids *pFA6a-HA::natMX6* or *pFA6a-GFP::kanMX6* (28), yielding strains CS38, CS38.7M, CS38.7D, LS37, JF5, CS81.7M, CS81.7D and NG96. To delete *pap1, trr1* and *pcr1* genes in *atf1-HA* strains, we transformed CS38, CS38.7M and CS38.7D strains with linear fragments containing ORF::*kanMX6* obtained by PCR amplification using ORF-specific primers and plasmid *pFA6a-kanMX6* as template as described previously (22,23), obtaining strains CS51 (*Δpap1 atf1-HA*) and its Atf1-HA phospho-mutants (CS51.7M and CS51.7D), CS62 (*Δtrr1 atf1-HA*) and CS52.7D (*Δpcr1 atf1.7D-HA*). We mutagenized *pap1* in Atf1-HA strain by crossing of strains IC2.C523D (*pap1.C523D*) and CS60 (*atf1-HA)* to obtain CS79.C523D strain. Cells were grown in rich medium (YE) or synthetic minimal medium (MM) as described previously (29).

H_2O_2 sensitivity assay - For survival on solid plates, *S. pombe* strains were grown, diluted and spotted on YE plates containing or not H_2O_2 at 1 or 2 mM as described previously (9).

RNA analysis by Northern Blot - Total RNA from *S. pombe* YE cultures was obtained, processed, and transferred to membranes (30). Membranes were hybridized with [α-32P] dCTP-labelled, *ctt1*, *hsp9*, *gpd1*, *srx1*, or *atf1* probe, containing the complete open reading frames. We used ribosomal RNA (*rRNA*) as a loading control.

S. pombe *TCA extracts and immuno blot analysis* - Modified trichloroacetic acid (TCA) extracts were prepared as previously described (23). Tagged or untagged Atf1 were immuno-detected with polyclonal anti-Atf1 (9), polyclonal anti-GFP (31) and with house-made monoclonal anti-HA antiserum (12CA5). Anti-Sty1 polyclonal antibody (32) and monoclonal anti-tubulin (Sigma) were used as loading controls.

RNA sequencing and analysis -Total RNA from *S. pombe* MM cultures, treated or not for

15 min with 1 mM H_2O_2, was obtained and processed as described previously (30). Libraries were prepared using the TruSeq Stranded mRNA Sample Prep Kit v2 (ref. RS-122-2101/2) according to the manufacturer's protocol. Briefly, 1 µg of total RNA was used for poly(A)-mRNA selection using streptavidin-coated magnetic beads and was subsequently fragmented to approximately 300bp. cDNA was synthesized using reverse transcriptase (SuperScript II, ref. 18064-014, Invitrogen) and random primers. The second strand of the cDNA incorporated dUTP in place of dTTP. Double-stranded DNA was further used for library preparation. dsDNA was subjected to A-tailing and ligation of the barcoded Truseq adapters. All purification steps were performed using AMPure XP beads. Library amplification was performed by PCR on purified library using the primer cocktail supplied in the kit. Final libraries were analyzed using Agilent DNA 1000 chip to estimate the quantity and check size distribution, and were then quantified by qPCR using the KAPA Library Quantification Kit (ref. KK4835, KapaBiosystems) prior to amplification with Illumina's cBot. Sequencing was done using the HiSeq2000, Single Read, 50 nts (v3). The raw reads were inspected using FastQC v0.11.2 (Fastqc -v0.11.2- http://www.bioinformatics.babraham.ac.uk/projects/fastqc/) for their quality and then mapped against the reference genome [*Schizosaccharomyces pombe* version EF2 from Ensembl corresponding to version ASM294v2 of PomBase 2015-04-21 (Schizosaccharomyces pombe, ASM294v2. http://fungi.ensembl.org/Schizosaccharomyces_pombe/Info/Index)] using Tophat version 2.0.14 (33)]. Read counts were counted using htseq-count tool (version 0.6.1p1) (34) with the option -m intersection-strict and -s reverse and normalized using the rlog function of DESeq2 package (35). The data discussed in this publication have been deposited in NCBI's Gene Expression Omnibus (36) and are accessible through GEO Series accession number GSE97057. Heatmap of rlog values was obtained by using the function pheatmap (1.0.8) from R package without reordering or clustering.

Chromatin immunoprecipitation - Cells were grown in minimal or rich media, as indicated, and chromatin isolation and immuno-precipitation was performed as described previously (12), with the following minor changes. Cell cultures were cross-linked for 10 min instead of 20 min. After chromatin isolation as indicated (12), specific antibodies [5 µl of anti-HA antiserum (12CA5), or 1 µl of polyclonal anti-Pap1 or anti-GFP] were added and incubation proceeded at room temperature rotating for 4 h to shorten the protocol (anti-HA or anti-Pap1).

Modelling and evaluation of the position of the six phospho sites in Atf1 - We modeled five potential conformations of the full-length sequence of Atf1 with the suit I-TASSER (25). Only two out of five had a bZIP domain in the C-terminal region, and out of these we selected the structure with Thr249 in a different domain than the rest of phosphorylable residues (Ser and Thr). We used MODELLER (37) to model the structure of the complex with DNA formed by Pcr1 and the bZIP domain of Atf1, based on the template conformation of a CREB-bZIP complex (38) [code 1DH3 of PDB (39)]. The complete model of Atf1 and Pcr1 was obtained by substituting the bZIP domain of the model selected from I-TASSER with the model of this region obtained with MODELLER. The complex was refined with ROSETTA (40).

Acknowledgments: The authors acknowledge the Genomic and the Bioinformatic Units of the Centre for Genomic Regulation (CRG, Barcelona, Spain) for their help in the performance and analysis of the RNA sequencing experiments. This work was supported by the Ministerio de Economía y Competitividad (Spain), PLAN E and FEDER (BFU2015-68350-P to EH), and by 2014-SGR-154 from Generalitat de Catalunya (Spain) to EH. LSM is recipient of a Juan de la Cierva post-doctoral contract, and CSC is recipient of a María de Maeztu pre-doctoral fellowship, both by the Ministerio de Economía y

Competitividad (Spain). EH is recipient of an ICREA Academia Award (Generalitat de Catalunya, Spain).

Conflict of interest: The authors declare that they have no conflicts of interest with the contents of this article.

Author contributions: CSC, EP, LSM and MC conducted most of the experiments. EP generated most of the strains expressing Atf1 mutants and the spots, Western and Northern blot experiments, CSC performed the RNA sequencing experiments and CSC and LSM the ChIP experiments. BO performed protein modeling experiments. CSC, EP, LSM, JA and EH designed the experiments and analyzed the results. EH wrote most of the paper.

REFERENCES

1. Weake, V. M., and Workman, J. L. (2010) Inducible gene expression: diverse regulatory mechanisms. *Nat Rev Genet* **11**, 426-437
2. Chen, D., Toone, W. M., Mata, J., Lyne, R., Burns, G., Kivinen, K., Brazma, A., Jones, N., and Bahler, J. (2003) Global transcriptional responses of fission yeast to environmental stress. *Mol.Biol.Cell* **14**, 214-229
3. Chen, D., Wilkinson, C. R., Watt, S., Penkett, C. J., Toone, W. M., Jones, N., and Bahler, J. (2008) Multiple pathways differentially regulate global oxidative stress responses in fission yeast. *Mol Biol Cell* **19**, 308-317
4. Shiozaki, K., and Russell, P. (1995) Cell-cycle control linked to extracellular environment by MAP kinase pathway in fission yeast. *Nature* **378**, 739-743
5. Samejima, I., Mackie, S., and Fantes, P. A. (1997) Multiple modes of activation of the stress-responsive MAP kinase pathway in fission yeast. *EMBO J.* **16**, 6162-6170
6. Millar, J. B., Buck, V., and Wilkinson, M. G. (1995) Pyp1 and Pyp2 PTPases dephosphorylate an osmosensing MAP kinase controlling cell size at division in fission yeast. *Genes Dev.* **9**, 2117-2130
7. Shiozaki, K., and Russell, P. (1996) Conjugation, meiosis, and the osmotic stress response are regulated by Spc1 kinase through Atf1 transcription factor in fission yeast. *Genes Dev.* **10**, 2276-2288
8. Wilkinson, M. G., Samuels, M., Takeda, T., Toone, W. M., Shieh, J. C., Toda, T., Millar, J. B., and Jones, N. (1996) The Atf1 transcription factor is a target for the Sty1 stress-activated MAP kinase pathway in fission yeast. *Genes Dev.* **10**, 2289-2301
9. Sanso, M., Gogol, M., Ayte, J., Seidel, C., and Hidalgo, E. (2008) Transcription factors Pcr1 and Atf1 have distinct roles in stress- and Sty1-dependent gene regulation. *Eukaryot Cell* **7**, 826-835
10. Lawrence, C. L., Maekawa, H., Worthington, J. L., Reiter, W., Wilkinson, C. R., and Jones, N. (2007) Regulation of Schizosaccharomyces pombe Atf1 protein levels by Sty1-mediated phosphorylation and heterodimerization with Pcr1. *J Biol Chem* **282**, 5160-5170
11. Castillo, E. A., Vivancos, A. P., Jones, N., Ayte, J., and Hidalgo, E. (2003) Schizosaccharomyces pombe cells lacking the Ran-binding protein Hba1 show a multidrug resistance phenotype due to constitutive nuclear accumulation of Pap1. *J Biol Chem* **278**, 40565-40572
12. Sanso, M., Vargas-Perez, I., Quintales, L., Antequera, F., Ayte, J., and Hidalgo, E. (2011) Gcn5 facilitates Pol II progression, rather than recruitment to nucleosome-depleted stress promoters, in Schizosaccharomyces pombe. *Nucleic Acids Res* **39**, 6369-6379
13. Brewster, J. L., and Gustin, M. C. (2014) Hog1: 20 years of discovery and impact. *Sci Signal* **7**, re7
14. Gaits, F., Degols, G., Shiozaki, K., and Russell, P. (1998) Phosphorylation and association with the transcription factor Atf1 regulate localization of Spc1/Sty1 stress-activated kinase in fission yeast [see comments]. *Genes Dev.* **12**, 1464-1473
15. Reiter, W., Watt, S., Dawson, K., Lawrence, C. L., Bahler, J., Jones, N., and Wilkinson, C. R. (2008) Fission yeast MAP kinase Sty1 is recruited to stress-induced genes. *J Biol Chem* **283**, 9945-9956
16. Eshaghi, M., Lee, J. H., Zhu, L., Poon, S. Y., Li, J., Cho, K. H., Chu, Z., Karuturi, R. K., and Liu, J. (2010) Genomic binding profiling of the fission yeast stress-activated MAPK Sty1 and the bZIP transcriptional activator Atf1 in response to H2O2. *PLoS One* **5**, e11620
17. Lawrence, C. L., Jones, N., and Wilkinson, C. R. (2009) Stress-induced phosphorylation of S. pombe Atf1 abrogates its interaction with F box protein Fbh1. *Curr Biol* **19**, 1907-1911
18. Ludlow, J. W., DeCaprio, J. A., Huang, C. M., Lee, W. H., Paucha, E., and Livingston, D. M. (1989) SV40 large T antigen binds preferentially to an underphosphorylated member of the retinoblastoma susceptibility gene product family. *Cell* **56**, 57-65

19. Paulo, E., Garcia-Santamarina, S., Calvo, I. A., Carmona, M., Boronat, S., Domenech, A., Ayte, J., and Hidalgo, E. (2014) A genetic approach to study H2O2 scavenging in fission yeast--distinct roles of peroxiredoxin and catalase. *Mol Microbiol* **92**, 246-257
20. Kon, N., Krawchuk, M. D., Warren, B. G., Smith, G. R., and Wahls, W. P. (1997) Transcription factor Mts1/Mts2 (Atf1/Pcr1, Gad7/Pcr1) activates the M26 meiotic recombination hotspot in Schizosaccharomyces pombe. *Proc Natl Acad Sci U S A* **94**, 13765-13770
21. Davidson, M. K., Shandilya, H. K., Hirota, K., Ohta, K., and Wahls, W. P. (2004) Atf1-Pcr1-M26 complex links stress-activated MAPK and cAMP-dependent protein kinase pathways via chromatin remodeling of cgs2+. *J Biol Chem* **279**, 50857-50863
22. Castillo, E. A., Ayte, J., Chiva, C., Moldon, A., Carrascal, M., Abian, J., Jones, N., and Hidalgo, E. (2002) Diethylmaleate activates the transcription factor Pap1 by covalent modification of critical cysteine residues. *Mol Microbiol* **45**, 243-254
23. Vivancos, A. P., Castillo, E. A., Biteau, B., Nicot, C., Ayte, J., Toledano, M. B., and Hidalgo, E. (2005) A cysteine-sulfinic acid in peroxiredoxin regulates H2O2-sensing by the antioxidant Pap1 pathway. *Proc Natl Acad Sci U S A* **102**, 8875-8880
24. Calvo, I. A., Garcia, P., Ayte, J., and Hidalgo, E. (2012) The transcription factors Pap1 and Prr1 collaborate to activate antioxidant, but not drug tolerance, genes in response to H2O2. *Nucleic Acids Res* **40**, 4816-4824
25. Yang, J., Yan, R., Roy, A., Xu, D., Poisson, J., and Zhang, Y. (2015) The I-TASSER Suite: protein structure and function prediction. *Nat Methods* **12**, 7-8
26. Sanso, M., Vargas-Perez, I., Garcia, P., Ayte, J., and Hidalgo, E. (2011) Nuclear roles and regulation of chromatin structure by the stress-dependent MAP kinase Sty1 of Schizosaccharomyces pombe. *Mol Microbiol* **82**, 542-554
27. Fernandez-Vazquez, J., Vargas-Perez, I., Sanso, M., Buhne, K., Carmona, M., Paulo, E., Hermand, D., Rodriguez-Gabriel, M., Ayte, J., Leidel, S., and Hidalgo, E. (2013) Modification of tRNA(Lys) UUU by elongator is essential for efficient translation of stress mRNAs. *PLoS Genet* **9**, e1003647
28. Bahler, J., Wu, J. Q., Longtine, M. S., Shah, N. G., McKenzie, A., III, Steever, A. B., Wach, A., Philippsen, P., and Pringle, J. R. (1998) Heterologous modules for efficient and versatile PCR-based gene targeting in Schizosaccharomyces pombe. *Yeast* **14**, 943-951
29. Alfa, C., Fantes, P., Hyams, J., McLeod, M., and Warbrick, E. (1993) *Experiments with Fission Yeast: A Laboratory Course Manual*, Cold Spring Harbor Laboratory, Cold Spring Harbor, N.Y.
30. Vivancos, A. P., Castillo, E. A., Jones, N., Ayte, J., and Hidalgo, E. (2004) Activation of the redox sensor Pap1 by hydrogen peroxide requires modulation of the intracellular oxidant concentration. *Mol Microbiol* **52**, 1427-1435
31. Calvo, I. A., Gabrielli, N., Iglesias-Baena, I., Garcia-Santamarina, S., Hoe, K. L., Kim, D. U., Sanso, M., Zuin, A., Perez, P., Ayte, J., and Hidalgo, E. (2009) Genome-wide screen of genes required for caffeine tolerance in fission yeast. *PLoS One* **4**, e6619
32. Jara, M., Vivancos, A. P., Calvo, I. A., Moldon, A., Sanso, M., and Hidalgo, E. (2007) The peroxiredoxin Tpx1 is essential as a H2O2 scavenger during aerobic growth in fission yeast. *Mol Biol Cell* **18**, 2288-2295
33. Trapnell, C., Pachter, L., and Salzberg, S. L. (2009) TopHat: discovering splice junctions with RNA-Seq. *Bioinformatics* **25**, 1105-1111
34. Anders, S., Pyl, P. T., and Huber, W. (2015) HTSeq--a Python framework to work with high-throughput sequencing data. *Bioinformatics* **31**, 166-169
35. Love, M. I., Huber, W., and Anders, S. (2014) Moderated estimation of fold change and dispersion for RNA-seq data with DESeq2. *Genome biology* **15**, 550
36. Edgar, R., Domrachev, M., and Lash, A. E. (2002) Gene Expression Omnibus: NCBI gene expression and hybridization array data repository. *Nucleic Acids Res* **30**, 207-210

37. Eswar, N., Webb, B., Marti-Renom, M. A., Madhusudhan, M. S., Eramian, D., Shen, M. Y., Pieper, U., and Sali, A. (2006) Comparative protein structure modeling using Modeller. *Current protocols in bioinformatics* **Chapter 5**, Unit 5 6
38. Schumacher, M. A., Goodman, R. H., and Brennan, R. G. (2000) The structure of a CREB bZIP.somatostatin CRE complex reveals the basis for selective dimerization and divalent cation-enhanced DNA binding. *J Biol Chem* **275**, 35242-35247
39. Rose, P. W., Beran, B., Bi, C., Bluhm, W. F., Dimitropoulos, D., Goodsell, D. S., Prlic, A., Quesada, M., Quinn, G. B., Westbrook, J. D., Young, J., Yukich, B., Zardecki, C., Berman, H. M., and Bourne, P. E. (2011) The RCSB Protein Data Bank: redesigned web site and web services. *Nucleic Acids Res* **39**, D392-401
40. Das, R., and Baker, D. (2008) Macromolecular modeling with rosetta. *Annu Rev Biochem* **77**, 363-382

FOOTNOTES

The abbreviations used are: H_2O_2, hydrogen peroxide; Pol II, RNA polymerase I; YE, rich medium; MM, minimal medium; OD, optical density; TCA, trichloroacetic acid; GFP, green fluorescent protein; MAP, mitogen activated protein; TF, transcription factor; bZIP, basic zipper.

FIGURE LEGENDS

FIGURE 1. The expression levels of Atf1 are not affected by stress when expressed from a constitutive promoter. (A) Schematic representation of HA-Atf1 showing the eleven canonical MAP kinase phospho sites. (B) YE cultures of strains 972 (WT), EP201 (*Δatf1* carrying an integrative empty vector, emp.) and EP203 (*Δatf1* carrying an integrative plasmid and expressing HA-Atf1 from the *sty1* constitutive promoter), were spotted on YE plates containing or not 2 mM H_2O_2 and incubated 3-4 days at 30ºC. (C) HA-Atf1 protein levels are not increased after stress imposition. Same cultures as in B were treated or not with 1 mM H_2O_2 for 15 min, TCA protein extracts were prepared and analyzed by Western blot using monoclonal antibody anti-HA, or polyclonal antibodies anti-Atf1. Antibodies against Sty1 were used as loading control. (D) Stress-dependent transcriptional analysis of *Δatf1* cells expressing the HA-Atf1 chimera. Total RNAs from cultures as in B were analyzed by Northern blot with probes for *hsp9, gpd1, ctt1, srx1* and *atf1*. *rRNA* is shown as a loading control. (E) Schematic representation of the positions of ten S/TP residues of Atf1 mutated to non-phosphorylatable (HA-Atf1.10M) or phospho-mimicking (HA-Atf1.10D) residues, expressed under the control of the constitutive *sty1* promoter. (F) Analysis of Atf1 phosphorylation in extracts from cells expressing HA-Atf1.10D or HA-Atf1.10M phospho mutants. YE cultures of strains 972 (WT), EP201 (*Δatf1* + emp.), EP203 (*Δatf1* + HA-Atf1), EP203.10D (*Δatf1* + HA-Atf1.10D) and EP203.10M (*Δatf1* + HA-Atf1.10M), were treated or not with 1 mM H_2O_2 during 15 min and processed as in Fig 1C. (G) *Δatf1* cells expressing the HA-Atf1.10D phospho mimicking mutant are not sensitive to peroxides. Same cultures as in F were spotted on plates containing 1 mM H_2O_2 as described in B.

FIGURE 2. Identification of two sets of stress genes differentially regulated by Sty1-Atf1. (A) Stress-dependent transcriptional analysis of Atf1 phospho mutants. YE cultures of strains 972 (WT), EP201 (*Δatf1* + emp.), EP203 (*Δatf1* + HA-Atf1), EP203.10D (*Δatf1* + HA-Atf1.10D) and EP203.10M (*Δatf1* + HA-Atf1.10M) were treated or not with 1 mM H_2O_2 for 15 min. Total RNA was analyzed by Northern blot as described in Fig 1D. (B) Expression of phospho mimicking HA-Atf1.10D suppresses the transcription defects of cells lacking Sty1. Cultures of strains 972 (WT), EP288 (*Δatf1 Δsty1* + emp.), EP303 (*Δatf1 Δsty1* + HA-Atf1), EP303.10D (*Δatf1 Δsty1* + HA-Atf1.10D) and EP303.10M (*Δatf1 Δsty1* + HA-Atf1.10M) were treated with 1 mM H_2O_2 during 15 min and total RNA was analyzed as described in Fig 1D. (C) Expression of HA-Atf1.10D suppresses the sensitivity to peroxides of cells lacking Sty1. Same cultures as in B were spotted on plates containing H_2O_2 as described in Fig 1B. (D) Representation of 246 genes whose transcript levels increase by at least two-fold in wild-type cells upon treatment with 1 mM H_2O_2 for 15 min. Total RNA from strains 972 (WT), AV18 (*Δsty1*), and EP303, EP303.10D and EP303.10M (*Δatf1 Δsty1* + HA-Atf1, HA-Atf1.10D and HA-Atf1.10M, respectively) was sequenced using Illumina technology and analyzed as described in Materials and Methods. Horizontal strips represent genes and columns represent untreated or treated conditions of the indicated strains. The log2 changes in expression, relative to the untreated wild-type sample, are color-coded as shown in the bar. Genes were hierarchically clustered based on the expression patterns of cells expressing HA-Atf1.10D. The relative positions of some representative genes (*srx1, ctt1, gpd1* and *hsp9*) are indicated on the right.

FIGURE 3. Recruitment of Atf1 to stress promoters is not dependent on its phosphorylation by Sty1. (A) Atf1-HA is recruited to the *ctt1* and *srx1* promoters after stress while it is constitutively bound to the *gpd1* and *hsp9* promoters. MM cultures of strains CS38 (a*tf1-HA*), CS38.7D (a*tf1.7D-HA*) and CS38.7M (*atf1.7M-HA*) were treated or not with 1 mM H_2O_2 for 5 min. ChIP experiments using anti-HA antibodies, coupled to quantification by real-time PCR, were performed using primers covering promoter

regions (*ctt1, srx1, gpd1* and *hsp9)*. Primers of an intergenic region were used as a negative control (control). (B, C) Stress-dependent phosphorylation of Atf1 promotes accumulation of Pol II at stress genes. YE cultures of strains JF5 (*rpb3-HA*), CS81.7D (*rpb3-HA atf1.7D*) and CS81.7M (*rpb3-HA atf1.7M*) were treated or not with 1 mM H_2O_2 during 15 min and CHIP assays were performed as in A using primers covering promoters (prom), open reading frames (ORF) or terminator regions (term) of the *gpd1* (B) and *ctt1* (C) genes. Data are presented as mean ± SEM. In (B, C): *P<0.05, **P<0.01, ***P<0.001 (Student's t-test)

FIGURE 4. Role of Pcr1 in the expression of Atf1-dependent genes. (A) H_2O_2-dependent expression of most stress genes, except *srx1,* is dependent on Pcr1. Total RNA from YE cultures of strains 972 (WT) and MS5 (*Δpcr1*), untreated or treated with 1 mM H_2O_2 for 15 min was analyzed by Northern blot as described in Fig 1D. (B) Binding of Pcr1 to stress promoters follows the same pattern than Atf1. MM cultures of strain NG96 (*pcr1-HA*) were treated or not with 1 mM H_2O_2 during 5 min and CHIP assays were performed as in Fig 3A. (C) The absence of Pcr1 abolishes the strong transcriptional activity of Atf1.7D-HA. YE cultures of strains 972 (WT), CS38.7D (*atf1.7D-HA*) and CS52.7D (*Δpcr1 atf1.7D-HA*) were treated with 1 mM H_2O_2 or not for 15 min and total RNA was analyzed as Fig 1D. (D) The recruitment of Atf1-GFP at most stress promoters, except *srx1,* is dependent on Pcr1. MM cultures of strains MS62 (*atf1-GFP*) and LS37 (*Δpcr1 atf1-GFP*) were treated or not with 1 mM H_2O_2 during 5 min and ChIP assays using anti-GFP antibodies were performed as in Fig 3A. Data are presented as mean ± SEM. In (B, D): *P<0.05 (Student's t-test).

FIGURE 5. Role of the TF Pap1 in the recruitment of Atf1 to one subset of stress promoters. (A) Pap1 is required for H_2O_2-dependent expression of *ctt1* and *srx1* but not for *gpd1* and *hsp9.* Cultures of strains 972 (WT), AV18 (*Δsty1*) MS98 (*Δatf1*) and AV25 (*Δpap1*) were treated or not with 1 mM H_2O_2 for 15 min. Total RNA was obtained and analyzed as in Fig 1D. (B) Deletion of Pap1 abolishes the activation of *srx1* and *ctt1* of cells expressing the phospho mimicking HA-Atf1.10D. YE cultures of strains 972 (WT), EP203.10D (*Δatf1* + HA-Atf1.10D), EP303.10D (*Δatf1 Δsty1* + HA-Atf1.10D) and PG125.10D (*Δatf1 Δpap1 Δsty1* + HA-Atf1.10D) were treated or not with 1 mM H_2O_2 for 15 min. Total RNA was obtained and analyzed as in Fig 1D. (C) The recruitment of Atf1-HA to the *ctt1* and *srx1* promoters is dependent on Pap1. MM cultures of strains CS51 (*Δpap1 atf1-HA*), CS51.7D (*Δpap1 atf1.7D-HA*) and CS51.7M (*Δpap1 atf1.7M-HA*) were treated or not with 1 mM H_2O_2 for 5 min and ChIP experiments were performed as in Fig 3A. (D) Oxidized/active Pap1 facilitates the H_2O_2-dependent recruitment of Atf1-HA to the *ctt1* and *srx1* promoters. MM cultures of strains CS62 (*Δtrr1 atf1-HA,* constitutively expressing oxidized nuclear Pap1) and CS79.C523D (*pap1.C523D atf1-HA,* expressing a constitutively reduced nuclear Pap1) were left untreated or treated with 1 mM H_2O_2 during 5 min. ChIP experiments were performed as in Fig 3A. (E) Pap1 binds to the *ctt1* and *srx1* promoters to the same extent in cells expressing or lacking Atf1. MM cultures of strains 972 (WT) and MS98 (*Δatf1*) were treated or not with 1 mM H_2O_2 for 5 min and ChIP experiments using anti-Pap1 antibodies were performed as in Fig 3A.

FIGURE 6. Ribbon plate of the predicted structure of unphosphorylated Atf1 (brown color) in complex with Pcr1 (orange) and a potential DNA (blue). The DNA binding domain of Atf1 (bZIP) is shown in magenta. Positions of the Cα atoms of six S/TP sites on the transactivation and intermediate domains are indicated in red spheres. Positions of the Cα atoms of Lys/Arg of these domains are shown in blue spheres.

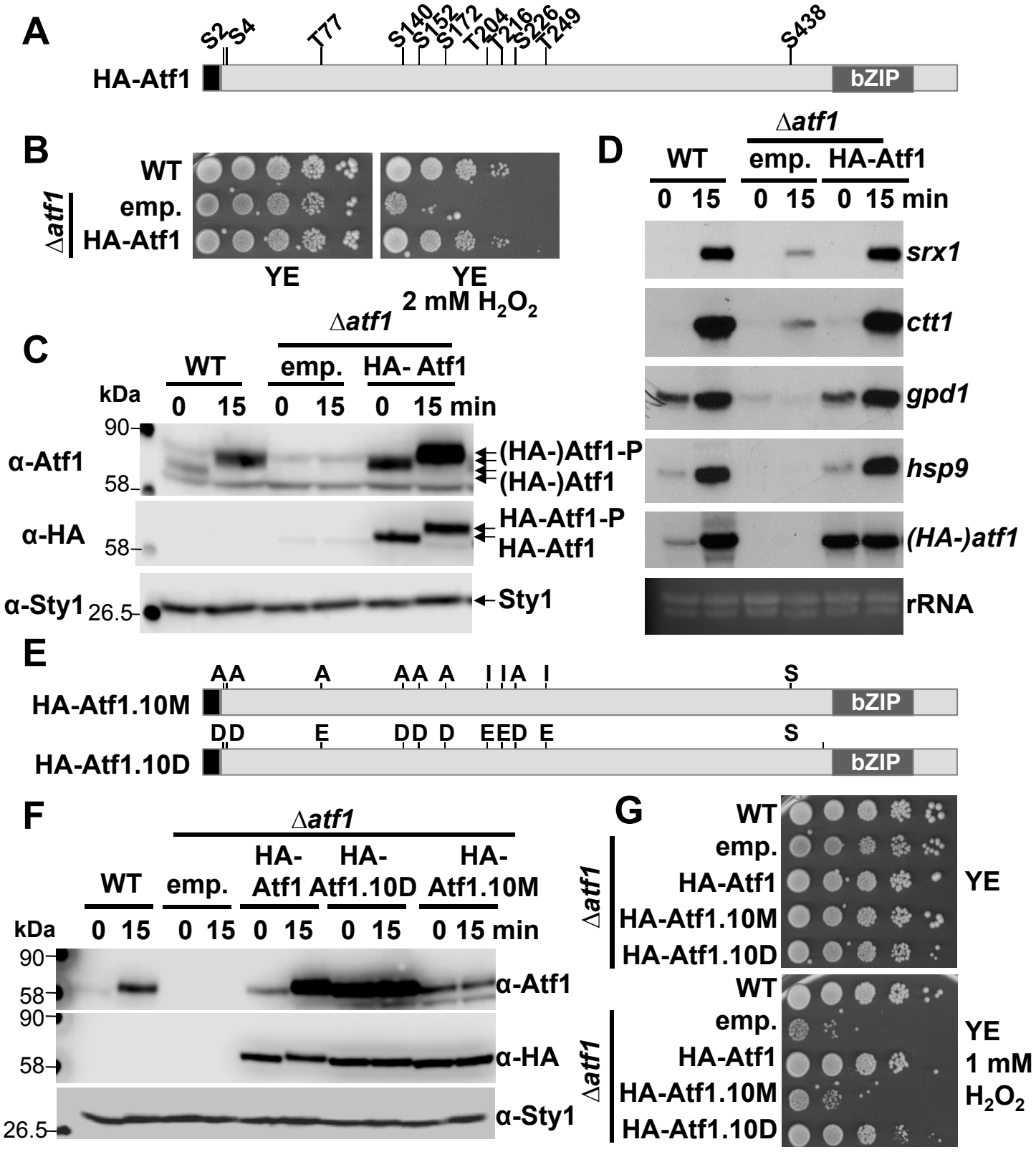

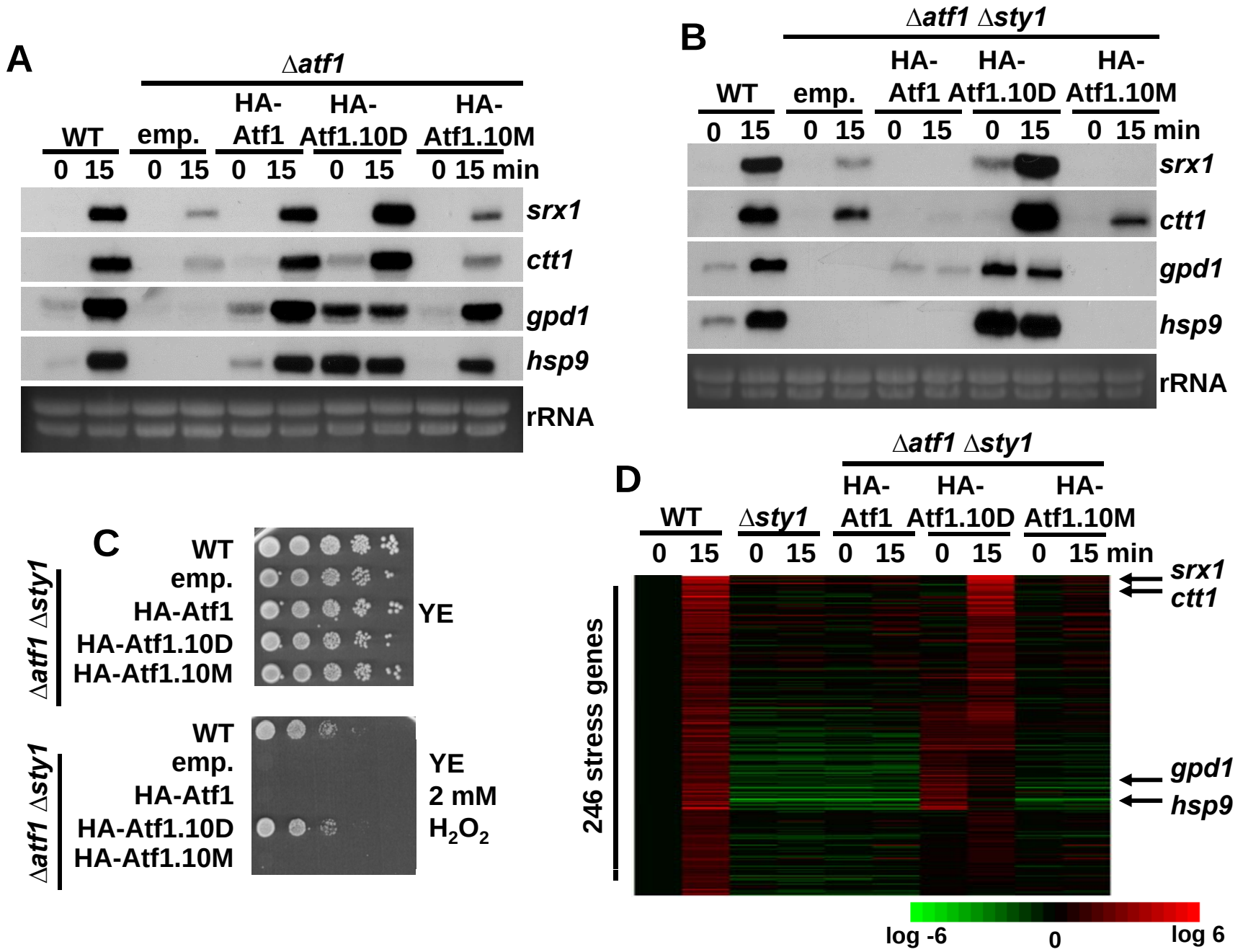

Salat et al Figure 2

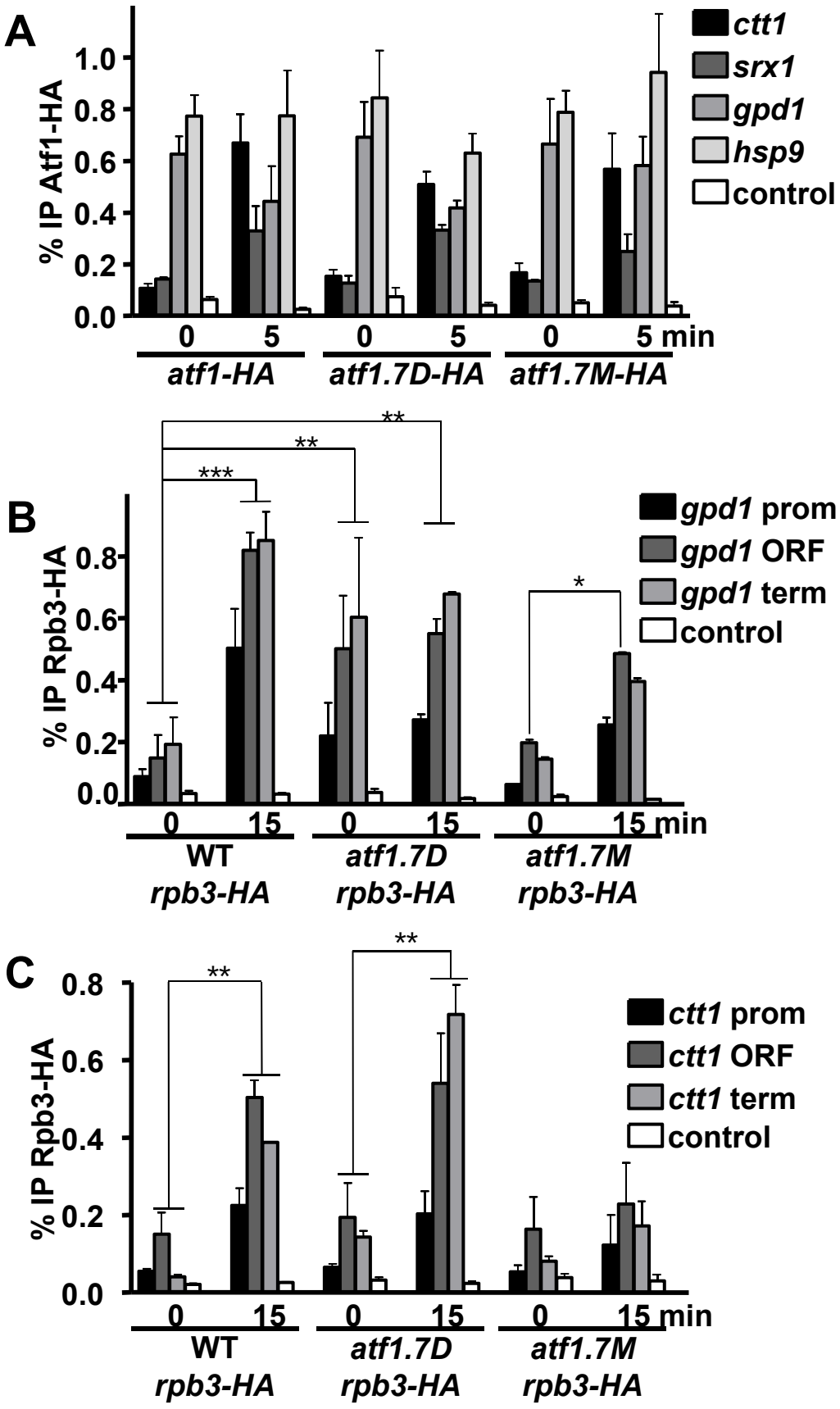

Salat et al Figure 3

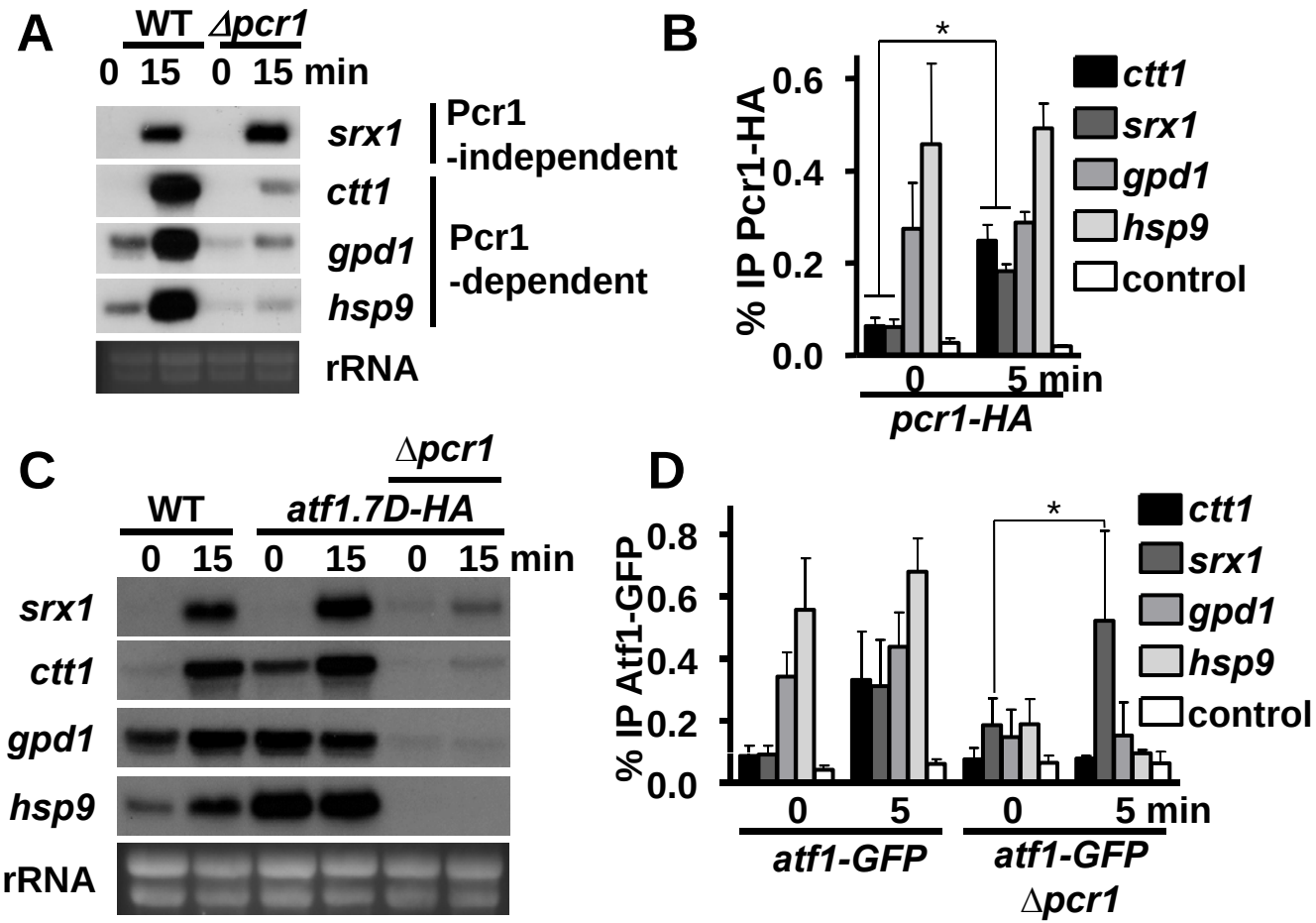

Salat et al Figure 4

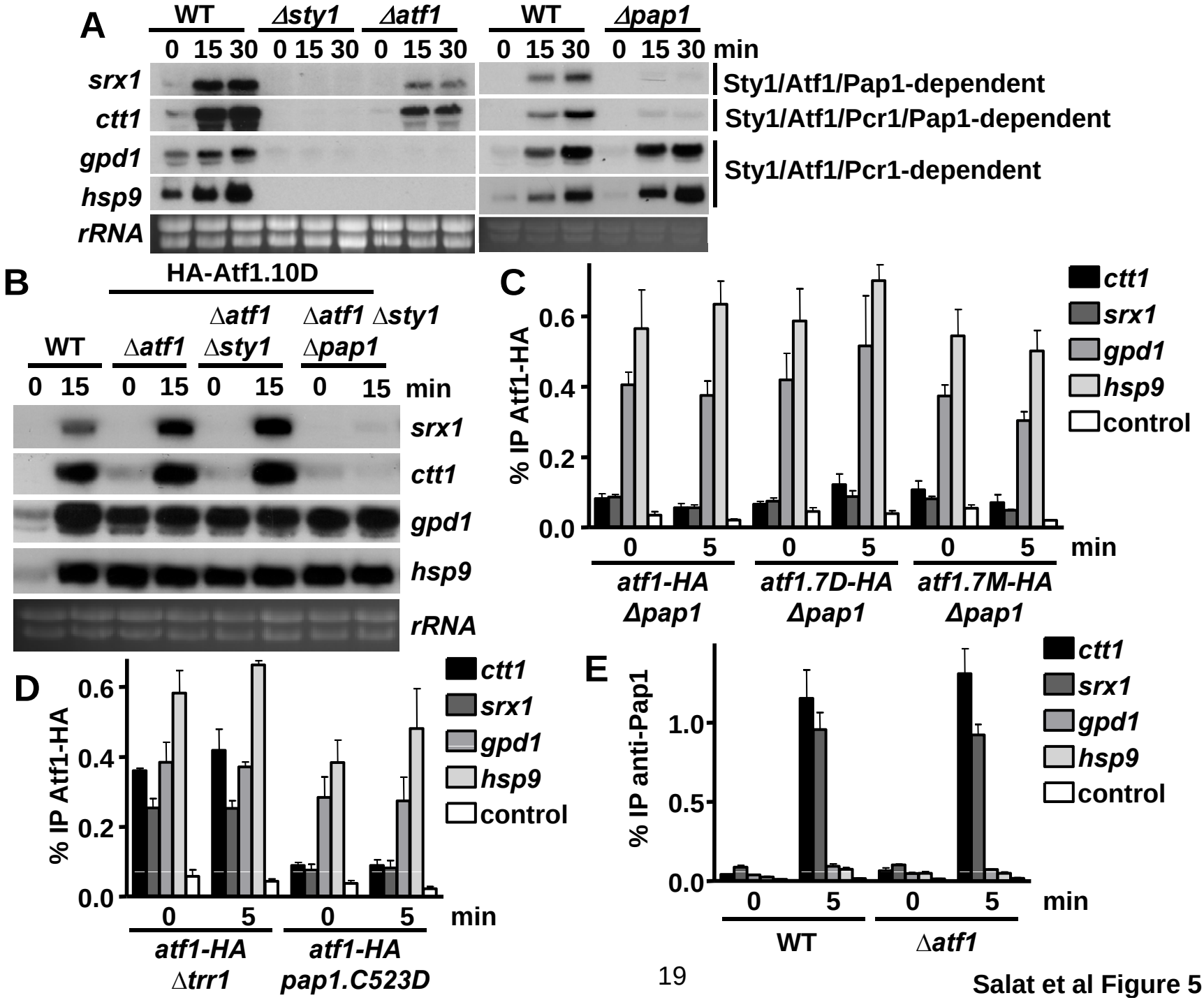

Salat et al Figure 5

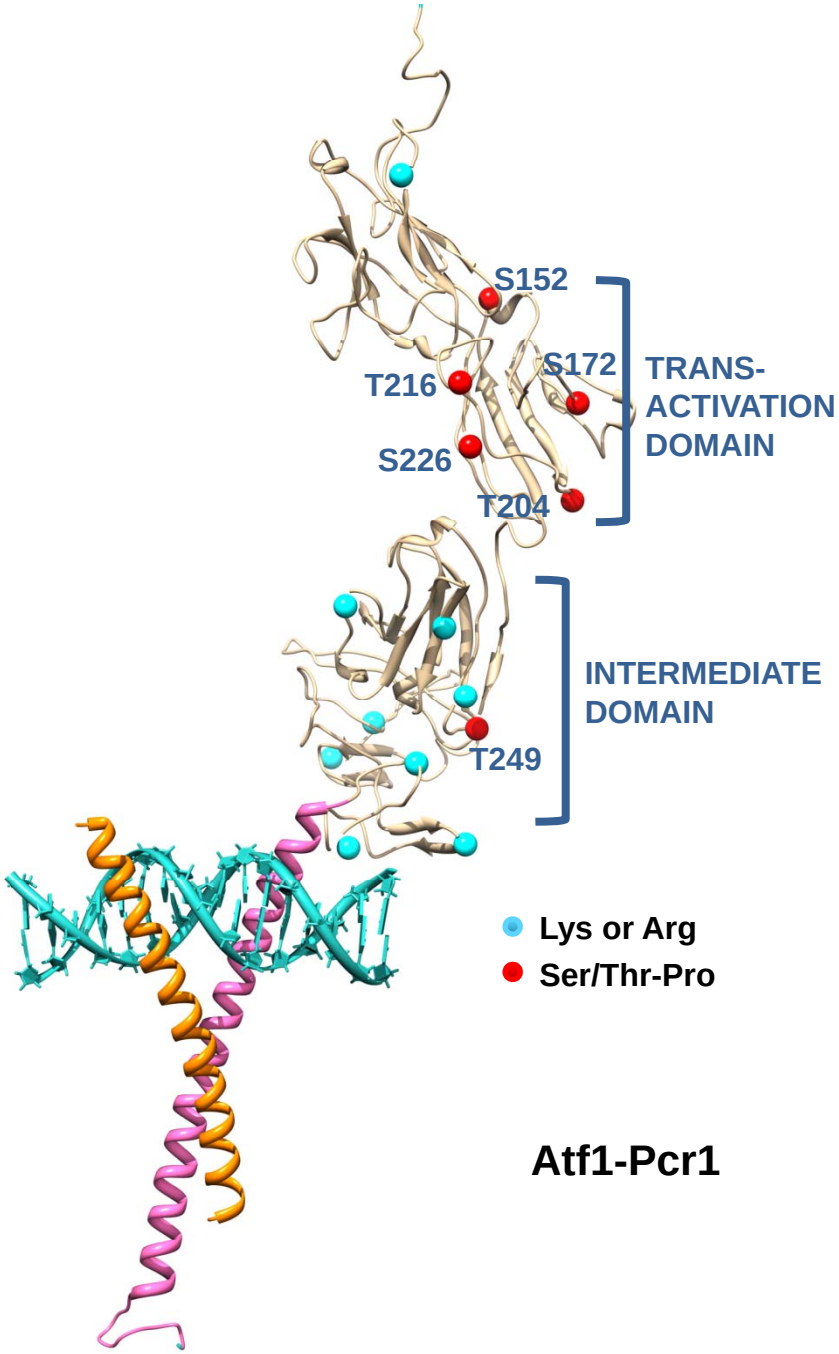

Salat et al Figure 6

Deciphering the role of the signal- and Sty1 kinase-dependent phosphorylation of the stress-responsive transcription factor Atf1 on gene activation

Clàudia Salat-Canela, Esther Paulo, Laura Sánchez-Mir, Mercè Carmona, José Ayté, Baldo Oliva and Elena Hidalgo

J. Biol. Chem. published online June 26, 2017
